Modeling anomalous superdiffusion

2007 J. Phys. A: Math. Theor. 40 11441

(http://iopscience.iop.org/1751-8121/40/38/001)

J. Phys. A: Math. Theor. **40** (2007) 11441–11452 doi:10.1088/1751-8113/40/38/001

Modeling anomalous superdiffusion

A Fischer[1], S Seeger[1], K H Hoffmann[1], C Essex[2] and M Davison[2]

[1] Institut für Physik, Technische Universität Chemnitz, D-09107 Chemnitz, Germany
[2] Department of Applied Mathematics, The University of Western Ontario, London, N6A, Canada

E-mail: hoffmann@physik.tu-chemnitz.de

Received 8 May 2007, in final form 15 July 2007
Published 4 September 2007
Online at stacks.iop.org/JPhysA/40/11441

Abstract
Continuous models for anomalous diffusion have previously been tested in the subdiffusive case by making comparisons to diffusion on a Sierpinski gasket. This paper extends this discussion to the superdiffusive case by comparing performance to diffusion on a tree model. Although there is reasonable agreement within limited regimes for all four models, one model, due to Compte and Jou, stands out as being consistently sound over all regimes studied.

PACS numbers: 47.27.tb, 05.40.Fb, 47.27.Eq

1. Introduction

Anomalous diffusion processes play an important role in physics, chemistry and biology. While normal diffusion is characterized by a second moment with a linear time dependence, anomalous diffusion shows a different time and space behavior. For these processes the second moment of the distribution scales like

$$\langle r^2(t)\rangle \propto t^{\frac{2}{d_w}}. \tag{1}$$

Processes with this scaling behavior occur in a variety of circumstances and have been observed with exponents $2/d_w$ smaller and larger than that for ordinary Brownian motion, where it is 1. For $d_w > 2$, we refer to the process as subdiffusive, because the particles diffuse slower than in regular diffusion; examples for such behavior occur for instance in charge carrier transport in amorphous semiconductors [1, 2], or the motion of a bead in a polymer network [3]. For $d_w < 2$ we refer to the process as superdiffusive, because the particles spread faster than in regular diffusion; examples for such behavior include relative diffusion of two particles in turbulent flows [4], diffusion of tracer particles in vortex arrays in a rotating flow [5] and layered velocity fields [6].

It is by no means clear that all those different phenomena are due to the same underlying mechanisms. One could not preclude that, for instance, in the case of the anomalous diffusion of adsorbed molecules at liquid surfaces [7] ($d_w < 2$) completely different mechanisms are

acting than for the case of diffusion on a fractal ($d_w > 2$). Nonetheless, most linear [8–12] or nonlinear [13] approaches for mathematically describing anomalous diffusion have either explicitly or implicitly been developed with a fractal structure in mind, which implicitly excludes the superdiffusive cases where $d_w < 2$.

The limitations of the different approaches in the subdiffusive case were discussed in a previous paper [14]. It showed that a number of proposed differential equations for anomalous diffusion on a fractal did not work. While these heuristic models exhibit the correct second moment behavior none match both asymptotically and at smaller scales. In subsequent papers, we took an entirely new approach [15, 16] with the aim of developing a direct mechanism to obtain governing equations.

After considering the subdiffusive case it is natural to consider anomalous diffusion in the superdiffusive regime. Modeling superdiffusive processes is of great importance from the point of technological application, where predictions of the density of the diffusing particles have to be made. We have looked previously at certain features of this regime [17–19], by using fractional diffusion equations, and found surprising features in the entropy production of such processes. They were intimately connected both to the dynamics and to the form of the probability density function (PDF).

While the diffusion on a Sierpinski gasket served as a prototypical model for subdiffusive behavior, we use a mesoscopic master equation based model [20, 21] here, rooted in the probabilistic description of dynamical maps, as our reference system for the superdiffusive case. That system is based on a master equation dynamics for the probability flow on a nested hierarchical set structure, which has been analyzed in depth. It will be referred to below as the tree-superdiffusion model. The PDF in d-dimensional spaces can be determined for it. We use that result to consider whether any of the continuum diffusion models suggested in the literature possess PDFs which are close, or equal, to the PDF obtained from the tree model.

We note that most of the continuum diffusion models are limited in their range of allowed d_w values, while the tree model is able to extent into the regime of turbulent diffusion. For the purpose of this analysis we limit $1 < d_w < 2$.

After a short presentation of the tree-superdiffusion model we introduce four continuum diffusion models. We show that they all show the proper time dependence of the second moment of their respective PDF, and trace this property back to the invariance of these model PDEs (partial differential equations) under a one-parameter scaling group. Then we focus on the form of the PDFs, as the different nature of the underlying diffusion processes will manifest itself in those. We then compare those PDFs with that from the tree superdiffusion in order to find parallels and differences. Our paper concludes with the interesting result that the model of Compte and Jou is the only one of the models surveyed to provide a good link with this dataset.

2. Tree-superdiffusion

The prototype model for superdiffusion to which we will compare the continuum models shows a distinctive tree structure. It belongs to a class of hierarchical models which play an important role in physics. They have been successfully used in the context of slowly relaxing systems like glasses, in the understanding of ageing phenomena in spin glasses, and in the analysis of complex dynamical maps. The tree model was suggested by Grossmann, Wegner and Hoffmann [20, 21] and is based on a master equation which transports probability on a nested set of intervals in a d-dimensional space with a tree structure [20]. It is able to produce a variety of different time dependences for the moments of the distribution [21]. This model can be used to mimic the transport of particles in a turbulent flow. In that case the nested

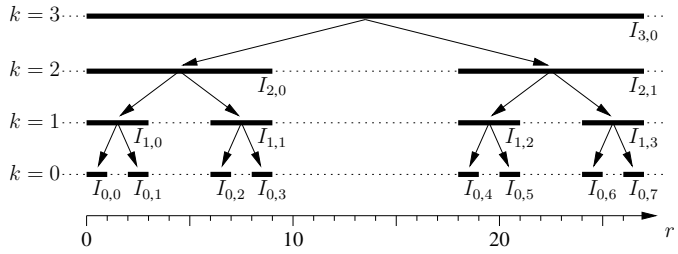

Figure 1. Geometric structure of a tree model with $z = 2$ and $\mu = 3$.

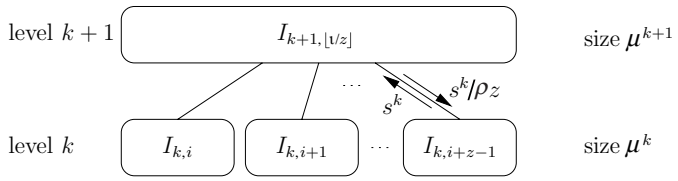

Figure 2. Brief description of the dynamics for the tree model.

intervals are representatives for the eddies of different sizes. For an appropriate choice of parameters one can obtain the desired time dependences, for example

$$\langle r^2 \rangle \propto t^3, \tag{2}$$

which would correspond to a fully developed turbulent diffusion which is faster than ballistic transport.

The geometric structure of a one-dimensional version of the model is shown in figure 1. Let us consider a set of intervals $I_{k,i}$ arranged in levels $k = 0, 1, \ldots$ and labeled $i = 0, 1, \ldots$ within each level. All intervals for a given level k are of the same size $l_k = \mu l_{k-1} = \mu^k l_0$, with the size of the lowest level chosen arbitrarily as $l_0 = 1$. A nested hierarchical structure is imposed by the condition that any intervals $I_{k,i}$ and $I_{k,j}$ with $i \neq j$ shall be disjoint and that an interval $I_{l,j}$ shall contain the intervals $I_{k,i}$ with $k \leqslant l$ and $i = jz^{l-k}, \ldots, (j+1)z^{l-k} - 1$. For instance, with the number of sub-intervals $z = 2$ as in figure 1 the interval $I_{2,1}$ must contain the intervals $I_{1,2}$, $I_{1,3}$, $I_{0,4}$, $I_{0,5}$, $I_{0,6}$ and $I_{0,7}$. This structure is self-similar in the sense that if $r \in I_{0,i}$ then $\mu^k r \in I_{k,i}$.

Now we recapitulate the dynamics of a random walk on this tree structure (see figure 2): the set of allowed positions of the walker is the intervals $I_{k,i}$. A walker may move upwards from interval $I_{k,i}$ to $I_{k+1,\lfloor i/z \rfloor}$ with the rate $\hat{w}_k = s^k \hat{w}_0$ where $\lfloor i/z \rfloor$ denotes the largest integer not greater than i/z. Similarly it may move downward to any of the intervals $I_{k-1,iz+j}$; $j = 0, 1, \ldots, z-1$ with a rate $\hat{\alpha}_k = s^{k-1}\hat{\alpha}_0/z$. The parameter s describes the rate scaling along the hierarchy, while the ratio $\rho = \hat{w}_0/\hat{\alpha}_0$ is the growth ratio. If $\rho > 1$, the upward transitions between adjacent level pairs dominate, if $\rho < 1$, walking downward is dominant. We chose the time unit such that $w_0 = 1$. The parameters (s, ρ, z, μ) define the model completely. Introducing the (overall) probability density $P_{k,i}(t)$ as the probability of the walker being in interval $I_{k,i}$ at time t, the master equation for the dynamic process reads

$$\frac{\mathrm{d}P_{k,i}}{\mathrm{d}t} = \begin{cases} -P_{0,i} + \dfrac{1}{\rho z} P_{1,\lfloor i/z \rfloor} & : k = 0 \\ s^{k-1} \displaystyle\sum_{j=0}^{z-1} P_{k-1,zi+j} - \left(\frac{s^{k-1}}{\rho} + s^k \right) P_{k,i} + \frac{s^k}{\rho z} P_{k+1,\lfloor i/z \rfloor} & : k > 0. \end{cases} \tag{3}$$

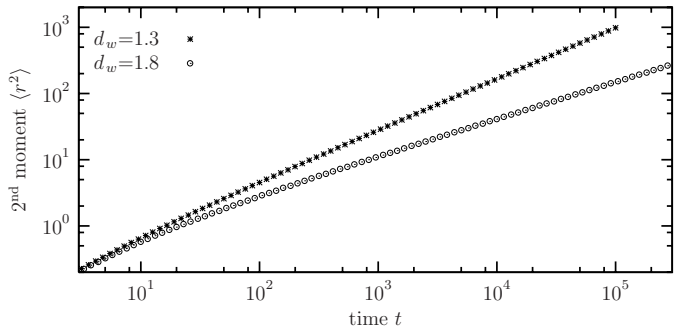

Figure 3. Second moments of the tree-diffusion PDFs for two different values of the random walk dimension $d_w = 1.3$ and $d_w = 1.8$ as used in the following comparisons. One can see that the scaling relation (1) is being fulfilled with only very little deviation for small times.

Initially, we assume all walkers concentrated in the leftmost interval at the lowest level

$$P_{k,i}(t = 0) = \delta_{k,0}\,\delta_{i,0}. \tag{4}$$

The time development of the dynamics is solved by considering the master equation (3) in matrix form $\dot{P}(t) = \mathbf{M}P(t)$ and diagonalizing the transition matrix $\mathbf{M}$. Afterward the probability distribution at any arbitrary time can be calculated by transforming the initial distribution into the eigenbasis of $\mathbf{M}$, utilizing the time and eigenvalue-dependent exponential decay, and transforming backwards.

We note that the tree model has a kind of fractional structure but stress that this fractional structure characterizes an additional dimension which is orthogonal to the radial distance on which the transport finally occurs. It is different from diffusion on fractal structures which are embedded in a higher dimensional space like the diffusion on a Sierpinski carpet.

While for a numerical solution the dimension of the master equation matrix has to remain finite one can go to infinite size systems by using a special technique for solving the master equation as given in [21]. Then, of course, the final solutions are in terms of infinite sums which can be approximated in the continuum limit by integral representations.

For the scaling features of the PDF the exact distribution of the particles inside the intervals $I_{k,i}$ is of no relevance [21]. Here a constant distribution in each interval is used. The overall $P(r, t)$ is obtained by summing up the contributions from all levels by using the intervals containing r. For the data shown in figure 3 we used $z = 2$, $\mu = 2$, $\rho = 9$ and $s = \mu^{-d_w}$.

Figure 3 shows the second moment of the PDF obtained within the above procedure for two different values of d_w, namely $d_w = 1.8$ and $d_w = 1.3$. While $d_w = 1.8$ is relatively close to regular diffusion, we expect to see clear deviations for $d_w = 1.3$.

In a log–log plot the scaling relation (1) should lead to straight lines. Figure 3 shows the expected scaling relation for tree-superdiffusion with only very small deviations for small times. These are due to the finite resolution of the model which become unimportant at the longer times we consider.

We now turn to the question, whether the tree-superdiffusion can be captured by continuum diffusion models.

3. Continuum models for tree-superdiffusion

We examine a number of distinct continuum diffusion equations [8–13] which have been proposed to describe anomalous diffusion. We discussed these models in the context of

modeling subdiffusive behavior as found in the diffusion on fractal structures. While some of those were constructed with the aim of modeling fractal diffusion, others had a wider range of application from the beginning. For details we refer the reader to [14]; here we discuss only those features and the respective background as needed.

The first important observation to be made is that all of the four continuum diffusion equations we will study can be written as a—not necessarily linear—integro-differential operator $\mathcal{O}$ acting on the PDF $P(r, t)$ which is intended to describe the underlying random walk process

$$\mathcal{O}P(r, t) = 0. \tag{5}$$

The second observation is that all four PDEs correctly reproduce the basic diffusion property (1). The underlying reason for that is that these equations are all invariant under a one-parameter similarity group, i.e. they are invariant under a scaling of the variables r and t:

$$r = \tilde{r}\lambda^{\beta}, \tag{6}$$

$$t = \tilde{t}\lambda, \tag{7}$$

where λ is a scaling factor and β is a value to be determined by the structure of $\mathcal{O}$. These equations introduce similarity variables, which are also invariant under the group. Here we choose a special one: $\eta \equiv r/t^{\beta}$, which is linear in r. For tree model computations we used fixed r, varying t to get different values of η.

Due to the invariance of the PDE in question we can look for solutions of the form $\mathcal{Q}(r/t^{\beta})$. However, as explained in [14] these would not satisfy the normalization requirement. Instead we need to search for solutions of the form

$$P(r, t) = t^{-\beta(1+a)}G(\eta), \tag{8}$$

where $G(\eta)$ satisfies an equation $\mathcal{B}_{\eta}\mathcal{G}(\eta) = 0$, with $\mathcal{B}_{\eta}$ being an auxiliary (integro-) differential operator in one independent variable. Assuming that $G(\eta)$ is positive in the full domain of η, one has

$$1 = \int_{\Sigma} P(r, t)cr^{a}\,\mathrm{d}r = t^{\beta(1+a)}\int_{\Sigma'} t^{-\beta(1+a)}G(\eta)c\eta^{a}\,\mathrm{d}\eta = \int_{\Sigma'} G(\eta)c\eta^{a}\,\mathrm{d}\eta, \tag{9}$$

where Σ is the domain of normalization in r space, Σ' is the corresponding domain in η space and $cr^{a}\,\mathrm{d}r$ is the volume element of a spherical shell at r with appropriate constants a and c.

Based on this form it follows that the mean-square displacement

$$\langle r^2\rangle = \int_{\Sigma} r^2 P(r, t)cr^{a}\,\mathrm{d}r = t^{2\beta}\int_{\Sigma'} G(\eta)c\eta^{a+2}\,\mathrm{d}\eta, \tag{10}$$

which reduces to relation (1) if we set $\beta = 1/d_w$ and the integral is taken as the constant of proportionality. Thus all the continuum diffusion equations satisfy the required scaling for the second moment of the radial distance due to the one-parameter scaling present.

We thus expect that there is a broad class of (integro-) differential equations which agree with (1), far exceeding those discussed above. To arrive at a specific equation, more conditions (heuristic, empirical, physical or otherwise) are necessary, naturally leading to the question posed here: which, if any, of the four equations to be introduced is able to model tree-superdiffusion appropriately.

That part of $P(r, t) = t^{-\beta(1+a)}G(\eta)$, which is invariant under the action of the one-parameter similarity group, $G(\eta)$, will be referred to as the auxiliary function or the G-density function (GDF), as it provides a time-independent representation of the PDF.

4. Modeling superdiffusion

In the following we present four different functions, $G_i(\eta)$, which are based on continuum diffusion PDEs. They will be used in our comparison with the PDF from the tree-superdiffusion model.

The GDFs of interest are

$$G_1(\eta) = N_1 \exp(-\kappa_1 \eta^{d_w}) \tag{11}$$

$$G_2(\eta) = N_2 H_{1,1}^{1,0}\left(\kappa_2 \eta^{d_w} \,\middle|\, \begin{matrix} \left(1-\frac{\phi}{d_w}, 1\right) \\ \left(\frac{1}{2}-\frac{\phi}{d_w}, d_w\right) \end{matrix}\right) \tag{12}$$

$$G_3(\eta) = N_3 H_{1,2}^{2,0}\left(\kappa_3 \eta^{d_w} \,\middle|\, \begin{matrix} \left(1-\frac{\phi}{d_w}, 1\right) & \\ \left(0, \frac{d_w}{2}\right), & \left(1-\frac{\phi}{d_w}, \frac{d_w}{2}\right) \end{matrix}\right) \tag{13}$$

$$G_4(\eta) = N_4 (1+\kappa_4 \eta^2)^{\frac{\phi}{d_w-2}}, \tag{14}$$

where $N_1, \ldots, N_4$ are suitably chosen normalization constants for the choice $a = 0$ and the normalization domain $0 < \eta < \infty$. This choice corresponds to the integration domain and a used in the tree-superdiffusion model. G_2 and G_3 are H-functions [22]. For details see also [23]. ϕ is a positive adjustable parameter, set greater than 0.01 to ensure convergence of H function implementations. We use it in the superdiffusion regime to adjust the distribution as well as possible to the observed data computed from tree-diffusion. Integrating over the normalization domain and using special features of the H-functions one obtains

$$N_1 = \frac{\kappa_1^{1/d_w}}{\Gamma(1+1/d_w)} \tag{15}$$

$$N_2 = \frac{d_w \kappa_2^{1/d_w} \Gamma\left(\frac{d_w-\phi+1}{d_w}\right)}{\Gamma\left(\frac{3}{2}-\frac{\phi}{d_w}\right)} \tag{16}$$

$$N_3 = \frac{d_w \kappa_3^{1/d_w} \Gamma\left(\frac{d_w-\phi+1}{d_w}\right)}{\Gamma\left(\frac{1}{2}\right)\Gamma\left(\frac{3}{2}-\frac{\phi}{d_w}\right)} \tag{17}$$

$$N_4 = 2\sqrt{\frac{\kappa_4}{\pi}} \frac{\Gamma\left(\frac{-\phi}{d_w-2}\right)}{\Gamma\left(\frac{-\phi}{d_w-2}-\frac{1}{2}\right)}. \tag{18}$$

The GDFs relate to a picture of diffusion on underlying fractal structures that imply diffusion under conditions of reduced connectivity compared to a full space. Thus they contain the fractal dimension, d_f, as a parameter, which has a physical meaning. In our approach above, this parameter, now renamed ϕ, becomes a mere parameter, open for adjustment in a fitting procedure, because the picture of an underlying fractal is not relevant to the case of superdiffusion. Also, the normalization, if carried out with a fractal structure in mind naturally leads to the choice $a = d_f - 1$, which is again different in our approach for the superdiffusive regime, where $a = 0$.

The first GDF (11) originates from an equation due to O'Shaughnessy and Procaccia [8, 9]:

$$\frac{\partial}{\partial t} P(r,t) = \frac{D_1}{r^{d_f-1}} \frac{\partial}{\partial r} r^{d_f-d_w+1} \frac{\partial}{\partial r} P(r,t). \tag{19}$$

It was most meticulously linked to the underlying structure of the Sierpinski gasket. Thus it was not aimed in the first instance at superdiffusion. However the equation retains the correct invariance properties into the superdiffusion domain.

Solving (19) leads to

$$P_1(r,t) = \frac{d_w \pi^{-d_f/2}\Gamma\left(\frac{d_f}{2}\right)}{2\Gamma\left(\frac{d_f}{d_w}\right)}(K_1 t)^{-\frac{d_f}{d_w}} \exp\left(-\frac{r^{d_w}}{K_1 t}\right), \tag{20}$$

from which we conclude that the normalization constant would be

$$\hat{N}_1 = \frac{d_w \pi^{-d_f/2}\Gamma\left(\frac{d_f}{2}\right)}{2\Gamma\left(\frac{d_f}{d_w}\right)} K_1^{-\frac{d_f}{d_w}}. \tag{21}$$

This constant is analogous to N_1 but differs by a factor of 2 as it is normalized over the full space, and it differs because $a = d_f - 1$ instead of 0.

The second GDF (12) is based on the solution to a fractional-order partial differential equation,

$$\frac{\partial^{\frac{1}{d_w}}}{\partial t^{\frac{1}{d_w}}} P(r,t) = -\frac{D_2}{r^{\frac{d_f}{d_w}-\frac{1}{2}}} \frac{\partial}{\partial r}\left(r^{\frac{d_f}{d_w}-\frac{1}{2}} P(r,t)\right), \tag{22}$$

proposed by Giona and Roman [10, 11] through various heuristic arguments. This PDE is solved by the PDF

$$P_2(r,t) = \frac{d_w \pi^{-d_f/2}\Gamma\left(\frac{d_f}{2}\right)}{2\Gamma\left(d_f + \frac{1}{2} - \frac{d_f}{d_w}\right)}(K_2 t)^{-\frac{d_f}{d_w}} H_{1,1}^{1,0}\left(\frac{r^{d_w}}{K_2 t}\,\middle|\, \begin{matrix}\left(1-\frac{d_f}{d_w}, 1\right) \\ \left(\frac{1}{2}-\frac{d_f}{d_w}, d_w\right)\end{matrix}\right). \tag{23}$$

This leads directly to

$$\hat{N}_2 = \frac{d_w \pi^{-d_f/2}\Gamma\left(\frac{d_f}{2}\right)}{2\Gamma\left(d_f + \frac{1}{2} - \frac{d_f}{d_w}\right)} K_2^{-\frac{d_f}{d_w}}, \tag{24}$$

which corresponds to N_2, but with the different specifications indicated above.

Our third GDF (13) comes from a fractional differential equation developed by Metzler *et al* [12]:

$$\frac{\partial^{\frac{2}{d_w}}}{\partial t^{\frac{2}{d_w}}} P(r,t) = -\frac{D_3}{r^{\frac{2d_f}{d_w}-1}} \frac{\partial}{\partial r} r^{\frac{2d_f}{d_w}-1} \frac{\partial}{\partial r} P(r,t), \tag{25}$$

where D_3 is an adjustable diffusion-like constant [23] inserted into the equation to allow comparison with arbitrary experiments.

Like the previous fractional order model, it was constructed by heuristic arguments which focused on achieving appropriate asymptotic behaviors. It, and its fractional order companion above, did well in the subdiffusive case. Both maintain the correct invariance properties in the superdiffusive domain.

Solutions of this differential equation can be obtained again in terms of H-functions [12, 23] to yield the PDF

$$P_3(r,t) = \frac{d_w \pi^{-d_f/2}}{2\Gamma\left(1 + \frac{d_f}{2} - \frac{d_f}{d_w}\right)}(K_3 t)^{-\frac{d_f}{d_w}} H_{1,2}^{2,0}\left(\frac{r^{d_w}}{K_3 t}\,\middle|\, \begin{matrix}\left(1-\frac{d_f}{d_w}, 1\right) & \\ \left(0, \frac{d_w}{2}\right), & \left(1-\frac{d_f}{d_w}, \frac{d_w}{2}\right)\end{matrix}\right). \tag{26}$$

Thus, the normalization constant is

$$\hat{N}_3 = \frac{d_w \pi^{-d_f/2}}{2\Gamma\left(1 + \frac{d_f}{2} - \frac{d_f}{d_w}\right)} (K_3)^{-\frac{d_f}{d_w}}, \tag{27}$$

paralleling N_3.

Our last GDF (14) is based on a differential equation suggested by Compte and Jou [13]:

$$\frac{\partial}{\partial t} P(r,t) = \frac{q D_4 d_f}{d_w + d_f - 2} \frac{\partial}{\partial r} r^{d_f - 1} \frac{\partial}{\partial r} (P(r,t))^{\frac{d_w + d_f - 2}{d_f}}, \tag{28}$$

where the constants D_4 and q are combined into one adjustable constant $K_4 \equiv q D_4$. In contrast to the others this differential equation is nonlinear and does not involve fractional order operators. It was deduced with arguments based on non-equilibrium thermodynamics.

The PDF solving (28) is then given in [13] as

$$P_4(r,t) = B K_4^{-\frac{d_f}{d_w}} \left(A^2 + \frac{r^2}{(K_4 t)^{\frac{2}{d_w}}} \right)^{\frac{d_f}{d_w - 2}}, \tag{29}$$

with A and B being suitably defined constants, implying a corresponding normalization constant. Note that this solution is different from that in the subdiffusive case [13, 14].

5. Fitting the model and comparison

In order to study the quality with which the different continuum approaches can model a case of superdiffusion, we compare the respective GDFs (equations (11)–(14)) to tree-superdiffusion.

We used two different parameter sets for determining the GDF of the tree model, leading to different random walk dimensions $d_w = 1.8$ describing diffusion relatively close to normal diffusion and $d_w = 1.3$ describing faster superdiffusion processes. In each case we look at the GDFs on a linear scale for analyzing the behavior in the domain near the peak of the distribution and look at the GDFs on a logarithmic scale to assess the behavior of the distribution's asymptotic tails.

Close to the peak we fitted the GDFs by least squares in the range of $\eta \in [1.0, \ldots, 3.0]$. For the asymptotic tails we obtained the best least-squares fit of the logarithm in the range of $\eta \in [5.0, \ldots, 10.0]$. The fitting error is minimized by adjusting the GDFs free model parameters indicated.

The random walk dimension d_w for all models is given by the scaling of the second moment of the probability density function and therefore needs to be equal for all models, in other words: it is a global parameter. The results are shown in figures 4–7.

As indicated, for the first GDF we take κ_1 (>0) and ϕ as adjustable parameters that are determined by a fit of G_1 to the data of the tree-superdiffusion. For small η, it turns out that G_1 is in good agreement with the reference solution in both cases. However, in figures 5 and 7 show that $G_1(\eta)$ has difficulties in the asymptotic regime as previously mentioned in [24]. Surprisingly, the agreement in the asymptotic case is better for $d_w = 1.3$ than for $d_w = 1.8$.

For $G_2(\eta)$ we used κ_2 and ϕ as adjustable constants too. As figures 5 and 7 show, the asymptotical behavior of this GDF in the superdiffusive case is not adequate. However it does more or less agree for small η in the case of $d_w = 1.8$, when η is not too close to the origin (i.e. $\eta \gtrsim 0.1$) . Notably, at the origin itself, there is a singularity. This anomaly appears for G_2 in all four comparison plots.

For $G_3(\eta)$ we used κ_3 and ϕ as fit parameters. Here the asymptotic behavior is not satisfied in the superdiffusive case. However, it turns out that $G_3(\eta)$ agrees well with the reference distribution for small η when $d_w = 1.8$, but not so well when $d_w = 1.3$ (see figures 4 and 6).

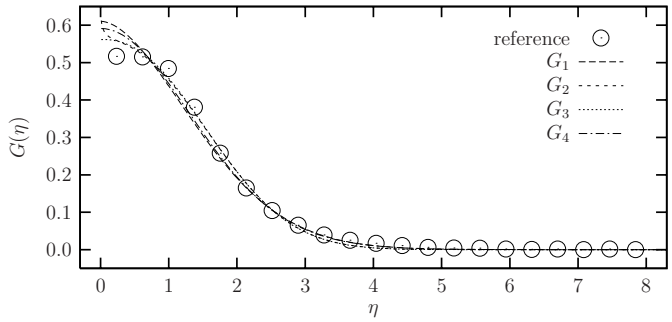

Figure 4. This is the GDF versus η in the case of $d_w = 1.8$ presented on a linear scale. The behaviors of the different models are compared near the peak by fitting on the interval $\eta \in [1.0, \ldots, 3.0]$. The reference model data are denoted by circles and reduced in number to facilitate clarity in viewing the other models. All of the models reproduce the tree-diffusion behavior acceptably for smaller η, with increasing deviation for decreasing η. For $\eta < 1$, G_2 begins to diverge as η vanishes. The other models slightly overestimate the tree data near the origin, but elsewhere are relatively accurate. At the origin, however, there is the notable exception that G_2 is singular.

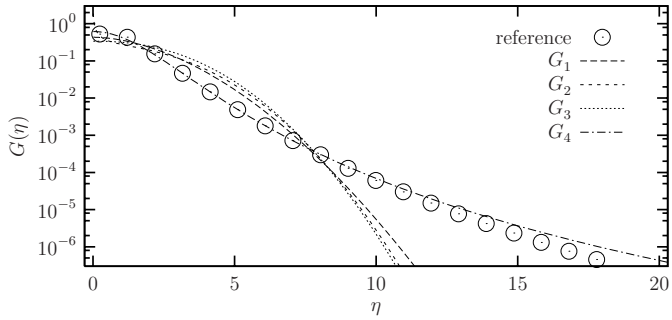

Figure 5. This is the GDF versus η in the case of $d_w = 1.8$ on a logarithmic scale. The fit has been performed on the interval $\eta \in [5.0, \ldots, 10.0]$ on logarithmic values to compare behaviors in the asymptotic tail. As one can see, the only model matching the tree-diffusion behavior is G_4.

In the latter case the function develops a pronounced maximum near $\eta = 1$ which is not seen in the reference case or in any other model.

For $G_4(\eta)$ we used κ_4 and ϕ as fit parameters. While in the subdiffusive case, the above approach was not so successful [14], it is by far the best in the superdiffusive case. In the case of small η it does agree as well as any other (see figures 4 and 6). In fact in the more extreme case of superdiffusion ($d_w = 1.3$) it improves. But in the asymptotic regime it is by far the best. It is the only one of the approaches discussed here that shows an acceptable agreement in the asymptotic range (see figures 5 and 7).

As one can see in figures 4–7 the overall behaviors of the different diffusion models are quite different from each other. In the asymptotic regime, for both d_w-values studied, the function G_4 is sub-exponential for large η, just as the reference data are. All other models have super-exponential tails (see figures 7 and 5). Overall, we find that the only model capable of reproducing the behavior of the tree-superdiffusion in both the peak and asymptotic regimes is G_4—the model of Compte and Jou.

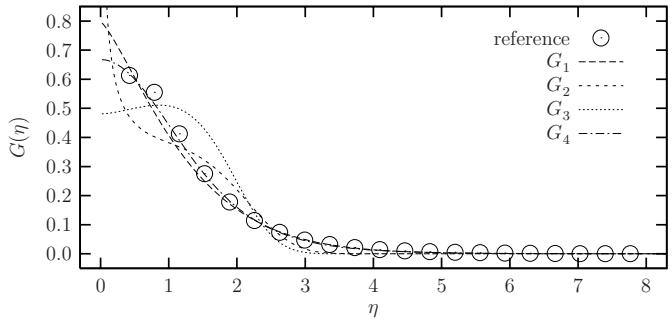

Figure 6. This is the GDF versus η in the case of $d_w = 1.3$ presented on a linear scale. The behaviors of the different models are compared near the peak by fitting on the interval $\eta \in [1.0, \ldots, 3.0]$. The reference model data are denoted by circles and reduced in number to facilitate clarity in viewing the other models. This case is further into the superdiffusion regime than the case of figure 4. The range of behaviors grows for small η, not only in magnitude but qualitatively as well. G_2 is singular at the origin, as before, but it also develops a pronounced wobble near $\eta = 1$. G_2 has a pronounced maximum near $\eta = 1$ and declines toward the origin. In contrast the performance of G_1 and G_4 improve relative to the previous case.

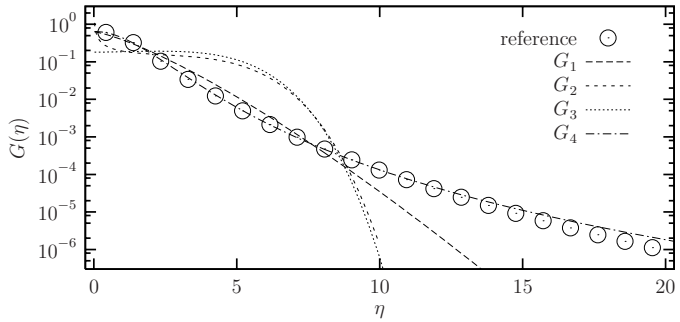

Figure 7. This is the GDF versus η in the case of $d_w = 1.3$ on a logarithmic scale. The fit has been performed on the interval $\eta \in [5.0, \ldots, 10.0]$ on logarithmic values to compare behaviors in the asymptotic tail. As one can see, the only model matching the tree-diffusion behavior is G_4.

6. Discussion and summary

We presented a hierarchical tree-based model used in a variety of applications, which provides a mesoscopic description of superdiffusion. The question we posed was, whether there exist known continuum diffusion models, which can adequately model the probability density function for superdiffusion as represented by the tree model.

All of the analyzed fractional diffusion equations have the correct scaling in the second moment of the probability density function in the superdiffusive domain, as we have shown (1). However, as already mentioned, complying with the scaling behavior is necessary but far from sufficient for a PDF to be adequate. There exist an infinite number of different probability distributions with the correct scaling behavior, even though most of them will not be physically sensible.

As pointed out above one expects that the underlying mechanisms generating subdiffusive and superdiffusive processes might be different. One can also envision that there are physically different mechanisms generating different superdiffusive processes. However the goal was to

make a specific comparison as has been previously carried out in the subdiffusive case in terms of the Sierpinski gasket. There is no particular reason to use that fractal for subdiffusion, but it provides a specific context for calculations and discussion. Correspondingly, we have used the tree-diffusion model as a specific context in which to study superdiffusion.

The respective continuum diffusion models were previously considered in the subdiffusive case. No suggestion is made that their originators have proposed that they be applicable in the superdiffusive regime (except Compte and Jou). Nonetheless, they are all clearly mathematically defined in the superdiffusive regime and they have all done surprisingly well given that they may have not been originally envisaged in that context.

Among them, the model of Compte and Jou stands out as the most consistently effective in both the peak and asymptotic regimes. It remains an interesting question why the model of Compte and Jou correctly reproduces the asymptotic behavior of the tree-superdiffusion, while it failed in reproducing the asymptotic behavior of the probability distribution produced by a random walk on a fractal [14]. At this point we can only speculate. One interesting fact is that Compte and Jou developed their diffusion equation based on very general arguments while the other diffusion equations are usually connected to the diffusion on fractals. The diffusive properties of the tree model are different from the usual fractal diffusion approach in that the additional dimension of the tree model enhances the transport rather than hinders it. This greater richness and the more general approach in the Compte and Jou diffusion equation might be an explanation for the good agreement.

References

[1] Scher H and Lax M 1973 Stochastic transport in a disordered solid: I. Theory *Phys. Rev.* B **7** 4491–502

[2] Scher H and Lax M 1973 Stochastic transport in a disordered solid: II. Impurity conduction *Phys. Rev.* B **7** 4502–19

[3] Amblard F, Maggs A C, Yurke B, Pargellis A N and Leibler S 1996 Subdiffusion and anomalous local viscoelasticity in actin networks *Phys. Rev. Lett.* **77** 4470–3

[4] Richardson L F 1926 Atmospheric diffusion shown on a distance–neighbour graph *Proc. R. Soc. Lond.* A **110** 709–37

[5] Weeks E R and Swinney H L 1998 Anomalous diffusion resulting from strongly asymmetric random walks *Phys. Rev.* E **57** 4915–20

[6] Zumofen G, Klafter J and Blumen A 1991 Trapping aspects in enhanced diffusion *J. Stat. Phys.* **65** 991–1013

[7] Bychuk O V and O'Shaughnessy B 1995 Anomalous diffusion at liquid surfaces *Phys. Rev. Lett.* **74** 1795–8

[8] O'Shaughnessy B and Procaccia I 1985 Analytical solutions for diffusion on fractal objects *Phys. Rev. Lett.* **54** 455–8

[9] O'Shaughnessy B and Procaccia I 1985 Diffusion on fractals *Phys. Rev.* A **32** 3073–83

[10] Giona Massimiliano and Eduardo Roman H 1992 Fractional diffusion equation on fractals: one-dimensional case and asymptotic behaviour *J. Phys. A: Math. Gen.* **25** 2093–105

[11] Eduardo Roman H and Giona Massimiliano 1992 Fractional diffusion equation on fractals: three-dimensional case and scattering function *J. Phys. A: Math. Gen.* **25** 2107–17

[12] Metzler R, Glockle W G and Nonnemacher T F 1994 Fractional model equation for anomalous diffusion *Physica* A **211** 13–24

[13] Compte A and Jou D 1996 Non-equilibrium thermodynamics and anomalous diffusion *J. Phys. A: Math. Gen.* **29** 4321–9

[14] Schulzky C, Essex C, Davison M, Franz A and Hoffmann K H 2000 The similarity group and anomalous diffusion equations *J. Phys. A: Math. Gen.* **33** 5501–11

[15] Essex C, Davison M, Schulzky C, Franz A and Hoffmann K H 2001 The differential equation describing random walks on the Koch curve *J. Phys. A: Math. Gen.* **34** 8397–406

[16] Davison M, Essex C, Schulzky C, Franz A and Hoffmann K H 2001 Clouds, fibres and echoes: a new approach to studying random walks on fractals *J. Phys. A: Math. Gen.* **34** L289–96

[17] Hoffmann K H, Essex C and Schulzky C 1998 Fractional diffusion and entropy production *J. Non-Equilib. Thermodyn.* **23** 166–75

[18] Essex C, Schulzky C, Franz A and Hoffmann K H 2000 Tsallis and Rényi entropies in fractional diffusion and entropy production *Physica* A **284** 299–308
[19] Li X, Essex C, Davison M, Hoffmann K H and Schulzky C 2003 Fractional diffusion, irreversibility and entropy *J. Non-Equilib. Thermodyn.* **28** 279–91
[20] Grossmann S, Wegner F and Hoffmann K H 1985 Anomalous diffusion on a selfsimilar hierarchical structure *J. Phys. Lett. France* **46** L575–83
[21] Hoffmann K H, Grossmann S and Wegner F 1985 Random walk on a fractal: eigenvalue analysis *Z. Phys.* B **60** 401–14
[22] Mathai A M and Saxena R K 1978 *The H-Function with Applications in Statistics and Other Disciplines* (New Delhi: Wiley Eastern Limited)
[23] Davison M 1995 Spatial and deterministic limits on randomness *PhD Thesis* University of Western Ontario
[24] Havlin S and Ben-Avraham D 1987 Diffusion in disordered media *Adv. Phys.* **36** 695–798